Supplementary Online Content

O'Neill J, Dong Z, Bansal R, et al. Proton chemical shift imaging of the brain in pediatric and adult developmental stuttering. *JAMA Psychiatry*. Published online November 23, 2016. doi:10.1001/jamapsychiatry.2016.3199

eAppendix

This supplementary material has been provided by the authors to give readers additional information about their work.

eAppendix.

(eIntroduction)

Motivation for ROI Selection Based on Prior Stuttering Neuroimaging Literature

Because prior imaging studies have consistently reported putative markers for stuttering in multiple neural systems distributed across the brain, we used a multi-planar chemical-shift imaging (MPCSI) variant of MRS that employs multivoxel arrays to interrogate wide expanses of brain simultaneously. MPCSI data were analyzed in two ways. First, conservatively, metabolites were examined at native MPCSI-resolution (1x1x1 cc, 1.6x1.6x1 cc with point-spread function, PSF) in pre-targeted regions-of-interest (ROIs; Table 2, eTable 1). ROIs were selected for prior neuroimaging evidence of stuttering-related effects, ready access to MPCSI sampling, and lower likelihood of susceptibility artifacts. Cortical ROIs included middle frontal cortex (MFC), inferior frontal cortex (IFC), insula, superior temporal cortex (STC), "frontoparietal-opercular central sulcal cortex" (FPO-CS; precentral cortex, post-central cortex and their *plis de passage*, subcentral and paracentral cortex), and inferior parietal cortex (IPC). Subcortical nuclear ROIs included caudate, putamen and thalamus. These ROIs have been implicated in stuttering by **volumetric MRI** (MFC, IFC;[1-2] STC;[1,3-4] FPO-CS;[1,4-6] IPC;[1,5] caudate;[6] putamen[1,4]), **task-fMRI** (MFC,[4,7-8] IFC,[4,7-11] insula,[4,7,9] STC,[4,8-9] FPO-CS,[4,8-10] IPC,[1,7] caudate,[7,8,10] putamen,[4,8,12] thalamus[4,10]), resting-state fMRI-- **rsfMRI** (MFC,[13] IFC,[13-14] STC,[13,15] FPO-CS,[13] putamen,[15] thalamus[14-15]), **$H_2{}^{15}O$-PET** (MFC,[16] IFC,[12,17-18] insula,[12,17-18] STC,[12,17-18] FPO-CS,[12,17,19] caudate,[12,16] thalamus[12,16-17]), and **^{18}FDG-PET** (IFC, IPC, caudate[20]). Varying across regions, effects have included higher or lower values of gray-matter volume or density, BOLD activation, BOLD connectivity, regional cerebral blood flow (rCBF), or glucose metabolic rate (GMR). Moreover, volumetric MRI[4] or DTI[5,21-24] have detected stuttering-related alterations (lower white-matter density, lower fractional anisotropy—FA) in the white matter subjacent to each of the above cortical ROIs. Thus, multiple streams of evidence support the *a priori* selection of each ROI. An additional voxel-based, data-driven approach interpolated data between MPCSI-voxels to derive statistical parametric maps at higher MRI resolution (1 mm^3). Both methods accounted for partial-volume effects and multiple statistical comparisons.

(eMethods)

[eFigure 1 and eTable 1]

Magnetic Resonance Post-Processing

MPCSI Post-Processing

Spectral post-processing[26-27] included spatial-filtering of the raw k-space MPCSI data with a Hamming window followed by slice-by-slice conversion to image space using 2D-Fourier transform. Time-domain echoes from the 8-coil array were combined as described[28-29] prior to 1D-Fourier transform into the frequency domain. Residual water was removed with singular-value decomposition.[30] Spectra were referenced to 2.01 ppm and phased to bring singlets into real mode. Model-based fitting identified NAA, creatine+phosphocreatine (Cr), Cho, and lipids, and integrated signal areas, correcting for receiver and transmitter gains. The fitting software was developed in-house in Matlab using a least-squares curve-fitting routine based on Gaussian lineshapes. For spectral quality control, we manually rejected voxels with strong lipid contamination, insufficient water-suppression, unresolved Cr and Cho, or full-width at half-maximum (FWHM) >16 Hz. Most spectra had FWHM <12 Hz. Peak-areas for NAA and Cho were normalized to Cr and arrayed into spectroscopic images. The PSF of MPCSI was calculated by independent simulation.[26]

Voxel-Based MRI/MPCSI Co-Processing

Using rigid, 6-parameter coregistration, the MPCSI-aligned localizers were mapped onto the FSPGR (after resampling to 1x1x1 mm^3). This yielded a transform ("D3" in Hao[26]) for later use. Using affine, 12-parameter coregistration (producing a "D4" transform) and non-linear fluid dynamics (producing "D5"[31]), the resampled FSPGR was brought into the coordinate space of a cross-participant T1-template. Independently, the gray-matter, white-matter, and CSF FSPGR subvolumes were coregistered into MPCSI-space using $D3^{-1}$. Convolution with the PSF then blurred the subvolumes to MPCSI resolution. These blurred subvolumes, together with the NAA/Cr and Cho/Cr spectroscopic images and the noise levels from fitting, were used to create new spectroscopic images with values of NAA/Cr and Cho/Cr partial-volume-corrected for gray matter and white matter as described.[26] Briefly, partial-volume-correction was performed by obtaining error-minimized estimates of the pure gray-matter and white-matter ratios across the entire data volume and then using these estimates and a linear regression model to calculate local metabolite ratios at each MPCSI voxel, based on gray-matter and white-matter content. Using D3, these spectroscopic images were transformed into resampled FSPGR-space. Using D4 and D5, they were transformed into T1-template coordinate space. Assignments of gray-matter or white-matter values of NAA/Cr and Cho/Cr were made for each voxel using nearest-neighbor analysis. Finally, MPCSI data were combined on cross-participant statistical parametric maps (SPMs).

Similar to standard fMRI post-processing, these SPMS are displayed at anatomical MRI resolution (1x1x1 mm^3), which is much higher than true MPCSI resolution. Such reconstruction of CSI data at MRI resolution has been employed previously.[26,32-33]

Similar to the smoothing kernel in fMRI, the MPCSI PSF in our procedure assures that assignment of metabolite ratios to anatomy is conducted at true MPCSI resolution, whereby the PSF acts as a spatial filter removing any artifactual metabolite variations at spatial frequencies higher than this resolution. Only after application of the PSF are MPCSI data resampled to anatomical MRI resolution and combined across participants into SPMs. Features smaller than an MPCSI voxel can emerge on these SPMs in the course of cross-subject computation. Similar to fMRI SPMs, MPCSI SPMs are interpreted statistically, i.e., where a metabolite effect on-average is observed within a sample, and not as single-subject spectroscopic images. As seen in Results in the main text, voxel-based findings obtained in this way were consistent with prior neuroimaging and present ROI-based findings, which used no interpolation.

Statistical Analyses

ROI-Based Analysis

Secondary investigations of regional metabolites assessed possible differences between child/adult and male/female subsamples. MANOVA for NAA/Cr and Cho/Cr was performed at each ROI with Diagnosis and Life-Stage (Child/Adult) as between-subjects variables. For ROIs with significant effects or interactions involving Life-Stage, and for metabolites with significant univariate effect, between-group comparisons were performed using protected *post-hoc* T-test, or ANCOVA in cases with a significant difference in one or more tissue-content variables between subsamples. Analogous analysis was conducted for male/female subsamples.

(eResults)

[eTable 2]

ROI-Based Analysis

Effects of Stuttering on Metabolites

To assess whether the NAA/Cr or Cho/Cr effects were driven by their denominator Cr, each of the above findings was retested substituting NAA/Cho for NAA/Cr and Cho/NAA for Cho/Cr, respectively. In the stuttering compared to control sample, NAA/Cho was lower in right IFC (-8.9%, $P = 0.007$), right inferior frontal white matter (-10.6%, $P = 0.001$), and right caudate (-13.5%, $P = 0.002$,); Cho/NAA was higher in right thalamus (+7.3%, $P = 0.02$), left STC (+7.5%, $P = 0.01$), right STC (+5.5%, $P = 0.08$ trend), left superior temporal white matter (+12.3%, $P < 0.001$), right superior temporal white matter (+6.9%, $P = 0.03$), and left putamen (+11.6%, $P = 0.009$). These ancillary results suggest strongly that the reductions in NAA/Cr and elevations in Cho/Cr in the various ROIs represent lower local levels of NAA and higher levels of Cho in stuttering, respectively, rather than effects of Cr. In left thalamus, where both NAA/Cr and Cho/Cr were elevated in stuttering, Cho/NAA was nearly significantly elevated (+4.9%, $P = 0.06$ trend), but NAA/Cho was trendwise reduced (-4.2%, $P = 0.10$ trend), consistent with elevation of both NAA and Cho in this nucleus in stuttering, independent of Cr.

Correlations of Metabolites with Severity

To assess whether NAA/Cr and/or Cho/Cr correlations were driven by Cr, each of the above findings was retested substituting NAA/Cho or Cho/NAA, respectively. We observed that NAA/Cho did not correlate significantly with Section I in either left ($r = +0.21$, $P = 0.21$) or right ($r = +0.26$, $P = 0.12$) thalamus; nor did Cho/NAA correlate significantly with Section I in left ($r = -0.22$, $P = 0.19$) or right ($r = -0.24$, $P = 0.15$) thalamus, consistent with Section I increasing with both NAA and Cho in the thalami, independent of Cr.

[eFigure 2 and eTable 3]

Voxel-Based Analysis

Correlations of Metabolite Ratios with Severity of Stuttering Symptoms

Significant voxel-based correlations of metabolite ratios with severity of stuttering symptoms (combined ACES/OASES Section I scores) within the stuttering sample are listed in eTable 3 (also see eFigure 2). Overlapping with ROI-based findings, the voxel-based analysis within the stuttering sample yielded positive correlations of NAA/Cr (left FDR-corrected $P < 0.001$; right $P = 0.006$) and Cho/Cr (left $P = 0.005$; right $P = 0.01$) with Section I scores in bilateral thalamus. The voxel-based analysis revealed numerous further significant correlations with symptoms within the stuttering sample. Among the findings in regions sampled by the ROI-based analysis, Section I score correlated positively with NAA/Cr in left MFC ($P = 0.005$) and left IFC ($P < 0.001$) and negatively with NAA/Cr in right insula and right STC ($P < 0.001$). Section I score correlated positively with Cho/Cr in left MFC ($P < 0.001$) and negatively with Cho/Cr in right insula and right STC ($P < 0.001$).

In regions not sampled by the ROI-based analysis, the voxel-based analysis yielded positive correlations of Section I with NAA/Cr in left ($P < 0.001$) and right ($P < 0.001$) FpC, right inferior temporal cortex ($P < 0.001$), left ($P = 0.006$) and right ($P = 0.001$) lingual cortex (i.e., lingual gyrus), right anterior and posterior middle cingulate cortices ($P < 0.001$), left PCC ($P = 0.01$), left ($P < 0.001$) and right ($P < 0.001$) deep prefrontal white matter, and left deep temporal white matter ($P = 0.005$). Section I correlated negatively with NAA/Cr in left ($P < 0.001$) and right ($P < 0.001$) latPC, bilateral amygdala ($P < 0.001$), and right forceps minor ($P < 0.001$). Section I correlated positively with Cho/Cr in bilateral FpC ($P < 0.001$), right inferior temporal cortex ($P < 0.001$), left ($P = 0.004$) and right ($P < 0.001$) lingual cortex, right anterior middle cingulate cortex ($P < 0.001$), and left ($P < 0.001$) and right ($P < 0.001$) deep prefrontal white matter. Section I scores correlated negatively with Cho/Cr in bilateral latPC ($P < 0.001$), bilateral amygdala ($P < 0.001$), right forceps minor ($P < 0.001$), right deep prefrontal white matter ($P < 0.001$), and left deep parietal white matter ($P < 0.001$). Thus, NAA/Cr and Cho/Cr correlations with stuttering symptoms were largely, though not completely, overlapping in distribution. They occurred in several regions where the effects of stuttering diagnosis on NAA/Cr and Cho/Cr had been observed, although in some additional regions as well.

Several exploratory correlations between metabolite ratios and scores on the other sections of ACES/OASES were significant after correction for multiple comparisons. For Section II (reactions to stuttering), these included positive correlations with NAA/Cr in right SFG and bilateral hippocampus. It also included positive correlations with Cho/Cr in bilateral frontal and parietal white matter and negative correlations with Cho/Cr in bilateral caudate. For Section III (communication in daily situations), significant metabolite correlations included positive correlations with NAA/Cr in bilateral frontal white matter. It also included positive correlations with Cho/Cr in bilateral frontal white matter and right lateral parietal cortex. For Section IV (quality-of-life), correlations were numerous. Positive correlations with NAA/Cr were found in bilateral PCC, left FpC, left MFC, and bilateral thalamus. Negative correlations with

NAA/Cr were found in bilateral superior parietal cortex, bilateral frontal and parietal white matter, bilateral PCC, right caudate, right STC, and bilateral amygdala. Positive correlations with Cho/Cr were found in bilateral frontal and parietal white matter, bilateral putamen, and bilateral internal capsule; there were negative correlations with Cho/Cr in bilateral IPC, bilateral PCC, bilateral amygdala, and right putamen. These exploratory findings were not further analyzed or interpreted.

[eTable 4]

ROI-Based Secondary Analysis: Effects on Regional Metabolite Ratios in Children *vs.* Adults

MANOVA revealed several significant main effects of, or interactions of group with, Life-Stage (Child, Adult). In right MFC we found a significant multivariate Diagnosis-by-Life-Stage interaction ($F_{2,63} = 3.2$, $P = 0.04$) in addition to a significant univariate main effect of Life-Stage for NAA/Cr ($F_{1,67} = 4.5$, $P = 0.04$), and a significant univariate Diagnosis-by-Life-Stage interaction for Cho/Cr ($F_{1,67} = 6.1$, $P = 0.02$). In right insula there was a significant multivariate Diagnosis-by-Life-Stage interaction ($F_{2,62} = 3.5$, $P = 0.04$) together with a significant univariate interaction for NAA/Cr ($F_{1,66} = 5.6$, $P = 0.02$). In right STC there was a significant multivariate effect of Life-Stage ($F_{2,73} = 5.2$, $P = 0.008$) with a significant univariate main effect of Life-Stage ($F_{1,77} = 9.9$, $P = 0.002$) and a significant Diagnosis-by-Life-Stage interaction ($F_{1,77} = 4.6$, $P = 0.04$) for NAA/Cr and a significant univariate main effect of Life-Stage for Cho/Cr ($F_{1,71} = 7.5$, $P = 0.008$). In right FPO-CS there was a significant multivariate Diagnosis-by-Life-Stage interaction ($F_{2,69} = 3.4$, $P = 0.04$) along with a significant univariate interaction for Cho/Cr ($F_{1,73} = 5.8$, $P = 0.02$). In right superior temporal white matter there was a significant multivariate main effect of Life-Stage ($F_{2,68} = 4.2$, $P = 0.02$) with the same significant univariate effects for NAA/Cr ($F_{1,72} = 8.4$, $P = 0.005$) and Cho/Cr ($F_{1,72} = 4.2$, $P = 0.04$). In right fronto-parietal operculum-central sulcal white matter there was a significant multivariate main effect of Life-Stage ($F_{2,69} = 4.6$, $P = 0.01$) with the same significant univariate effects for NAA/Cr ($F_{1,73} = 4.5$, $P = 0.04$) and Cho/Cr ($F_{1,73} = 8.9$, $P = 0.004$). In right inferior parietal white matter there was a significant multivariate Diagnosis-by-Life-Stage interaction ($F_{2,59} = 3.7$, $P = 0.03$) with the same significant univariate interactions for NAA/Cr ($F_{1,58} = 4.2$, $P = 0.05$) and Cho/Cr ($F_{1,58} = 6.3$, $P = 0.02$). In left thalamus there were a significant multivariate main effect of Life-Stage ($F_{2,71} = 5.5$, $P = 0.006$) and a significant multivariate Diagnosis-by-Life-Stage interaction ($F_{2,71} = 3.6$, $P = 0.03$) with a significant univariate main effect of Life-Stage ($F_{1,75} = 10.9$, $P = 0.002$) and a significant Diagnosis-by-Life-Stage interaction ($F_{1,75} = 6.6$, $P = 0.01$) for NAA/Cr and a significant univariate main effect of Life-Stage for Cho/Cr ($F_{1,75} = 4.3$, $P = 0.04$) for Cho/Cr. Similarly, in right thalamus there were a significant multivariate main effect of Life-Stage ($F_{2,73} = 5.2$, $P = 0.008$) and a significant multivariate Diagnosis-by-Life-Stage interaction ($F_{2,73} = 5.5$, $P = 0.005$) with a significant univariate main effect of Life-Stage ($F_{1,71} = 10.1$, $P = 0.002$) and a significant Diagnosis-by-Life-Stage interaction ($F_{1,71} = 11.5$, $P = 0.001$) for NAA/Cr and a significant univariate main effect of Life-Stage for Cho/Cr ($F_{1,77} = 5.6$, $P = 0.02$) for Cho/Cr.

In protected *post-hoc* testing comparing stuttering to control participants in child and adult subsamples separately, the following significant results were found in T-test or ANCOVA covarying one or more tissue-content variables, as appropriate. First, it

was determined that the following between-group differences were significant for children only, but not for adults: NAA/Cr in right IFC ($t_{37.1}$ = -2.4, P = 0.02, -9.7% ["-" means lower in the Stuttering sample]), NAA/Cr in left insula (t_{36} = 2.0, P = 0.05,+8.9%), NAA/Cr ($t_{34.1}$ = 2.9, P = 0.006,+15.5%) and Cho/Cr ($t_{36.9}$ = 3.2, P = 0.003,+15.4%) in left thalamus, and NAA/Cr ($t_{35.1}$ = 2.7, P = 0.009,+15.5%) and Cho/Cr ($t_{37.8}$ = 3.3, P = 0.002,+15.5%) in right thalamus. Second, the following between-group differences were significant for adults only, but not for children: NAA/Cr ($t_{35.1}$ = 2.3, P = 0.03,+15.3% ["+" means higher in the Stuttering sample]) and Cho/Cr (t_{38} = 3.1, P = 0.004,+20.5%) in right STC. Third, the following differences between children and adults were significant for healthy controls only, but were missing in stuttering subjects: NAA/Cr in right STC ($F_{1,39}$ = 4.7, P = 0.04, covary ROI, +21.4% ["+" means higher in children]), Cho/Cr in right FPO-CS ($F_{1,37}$ = 5.8, P = 0.02, covary ROI, +18.0%), NAA/Cr (t_{35} = 2.0, P = 0.05,+9.1%) and Cho/Cr ($t_{34.8}$ = 3.0, P = 0.005,+17.1%) in right fronto-parietal operculum-central sulcal white matter, and NAA/Cr ($F_{1,26}$ = 4.0, P = 0.05, covary white matter, +13.2%) and Cho/Cr ($F_{1,26}$ = 4.3, P = 0.05, covary white matter, +17.4%) in right inferior parietal white matter. Finally, the following differences between children and adults were significant for stutterers only: NAA/Cr in right MFC ($F_{1,33}$ = -6.4, P = 0.02, covary ROI and white matter, -15.6% ["-" means lower in children]), NAA/Cr in left insula ($F_{1,30}$ = 6.3, P = 0.02, covary white matter, +15.6%), NAA/Cr in left thalamus ($F_{1,36}$ = 6.3, P = 0.02, covary ROI, white matter, and gray matter, +20.8%), and NAA/Cr ($t_{39.7}$ = 4.2, P < 0.001, +23.3%) and Cho/Cr ($t_{35.5}$ = 2.7, P = 0.01, +11.9%) in right thalamus.

[eTable 5]

ROI-Based Secondary Analysis: Effects on Regional Metabolite Ratios in Males *vs.* Females

MANOVA revealed a few significant effects involving Sex. In right STC there was a significant multivariate main effect of Sex ($F_{2,78}$ = 4.2, P = 0.02) and a significant univariate main effect of Sex on NAA/Cr ($F_{1,77}$ = 7.9, P = 0.006). In right putamen there was a significant multivariate main effect of Sex ($F_{2,69}$ = 3.4, P = 0.04) and a significant univariate main effect of Sex on Cho/Cr ($F_{1,73}$ = 5.4, P = 0.02). And in right right fronto-parietal operculum-central sulcal white matter there were significant multivariate ($F_{2,69}$ = 3.7, P = 0.03) and univariate ($F_{1,73}$ = 7.4, P = 0.008) main effects of Sex on NAA/Cr.

In protected *post-hoc* tests comparing stuttering to control participants in male and female subsamples separately, the following significant results were found in T-test or ANCOVA covarying one or more tissue-content variables. First, it was determined that one between-group difference, that for NAA/Cr in right STC ($F_{1,31}$ = 5.2, P = 0.03, covary ROI, +8.9% ["+" means higher in the Stuttering sample]) was significant for females only. Second, two effects of Sex—that for NAA/Cr in right STC ($t_{29.9}$ = 2.9, P = 0.006, +13.3% ["+" means higher in females]) and that for Cho/Cr in right putamen ($t_{32.1}$ = -2.3, P = 0.03, -10.4%)-- were significant for people who stutter only.

(eDiscussion)

Metabolite Findings in Individual Brain Regions, Comparison with Prior Literature

In addition to the analysis in terms of functional brain networks and circuits undertaken in the main text, we present here an interpretation of the observed diagnostic effects of stuttering in terms of individual brain regions. **MFC** mediates cross-temporal contingencies.[35] Our fMRI study[7] observed below-normal BOLD activation in left MFC during context-dependent adaptation in stuttering. We interpreted this result as inadequate readiness of stuttering speakers to execute a sequence of motor responses. Other prior work in MFC has demonstrated effects of stuttering on gray-matter volume,[1,3] BOLD response,[4,8] and BOLD connectivity.[13] Bilateral middle frontal white matter also has lower FA in stutterers.[21] In the present study, voxel-based analysis showed elevated Cho/Cr in the stuttering sample in right MFC and elevated NAA/Cr in left middle frontal white matter, perhaps reflecting local elevated membrane metabolism and elevated neuronal density or metabolic activity, respectively.

Right **IFC** is thought to support speech rhythm[36] as part of an auditory pacing network.[37-39] Long-range fibers impinging upon or exiting from IFC are associated with motor timing, impulse control, and speech processing.[40] IFC is a frequent site of alterations in stuttering, effects being recorded with volumetric MRI,[1,5] task-fMRI,[4,7-11,41] rsfMRI,[13-14] $H_2{}^{15}O$-PET,[16-17] and ^{18}FDG-PET.[20] FA is also below-normal in bilateral inferior frontal white matter in stuttering.[21-22] Right IFC over-activation is viewed by some as a physiological hallmark of stuttering.[42] It is thought to represent compensation for speech deficits;[4] right IFC, for example, is activated during light stuttering, but not during heavy stuttering,[8] and treatment increases right IFC activation.[8,11] The present study detected below-normal NAA/Cr in right IFC and inferior frontal white matter with ROI- and voxel-based approaches. Right IFC NAA/Cr increased with severity of stuttering symptoms, in keeping with the compensation hypothesis (i.e., reduction of NAA/Cr within people who stutter helps mitigate symptoms).

The **insula** is suspected of involvement in most speech functions.[43] Insular activation occurs during pseudoword pronunciation, singing, swallowing, speaking aloud, and breathlessness, but not during silent speech.[44] The insula, together with right IFC, helps process vocal fundamental frequencies and prosody.[44] Right insula is also activated in chronic anxiety.[45] In prior investigations, effects of stuttering on the insula have been found with task-fMRI[4,7,9] and $H_2{}^{15}O$-PET.[12,17-18] Elevated FA was detected in insular white matter, one of very few cases of above-normal FA in stuttering.[22] In the voxel-based analysis in our stuttering sample, NAA/Cr and Cho/Cr were elevated in left insula, Cho/Cr was diminished in right insula, and NAA/Cr was diminished in right insular white matter. Thus, neuronal and glial density and metabolic activity, including membrane metabolism, may be elevated in the left insula and diminished in the right insula in stuttering.

STC may be involved in conscious verbal self-monitoring in support of automatic speech production.[46] It also detects mismatch between actual and anticipated auditory feedback[47] and has been implicated in auditory pacing.[38] STC white matter,

including parts of the superior longitudinal fasciculus and the fasciculus arcuate in the left hemisphere, helps mediate syntax and phonology.[48-50] The STC also subserves speech imitation and motor control.[40] Underconnectivity of temporal auditory cortex and disconnection between left STC and left IFC have been proposed to drive stuttering.[51] Neuroimaging alterations are regularly reported in STC in stuttering. These include effects with volumetric MRI,[1,3-4] task-fMRI,[4,8] rsfMRI,[13,15] and PET.[12,17,20,42-43] There are multiple findings of below-normal FA in superior temporal white matter.[5,21-23] In our study, elevated Cho/Cr was measured in stuttering participants in bilateral STC and superior temporal white matter in ROI- and voxel-based analyses. This may reflect overactive membrane metabolism (synthesis or degradation) associated with stuttering-related dysfunction in this region.

Our **FPO-CS** ROI comprises primary motor cortex, primary somatosensory cortex, and the subcentral and paracentral gyri that connect them. Primary motor cortex is the final cortical output for speech behavior,[52] and somatosensory cortex is the first stage for proprioceptive input from speech organs.[53] In the left hemisphere, altered timing in these structures is thought to affect articulatory preparation for speech prosody generation.[16-17] Defects in white matter underlying FPO-CS may delay signal transmission between movement-planning, movement-execution, and sensory cortices, thus impairing fluent speech.[40] An abundance of prior evidence suggests alterations in stuttering in FPO-CS and its white matter from MRI,[1,4-5] task-fMRI,[4,6,8-10] rsfMRI,[13] $H_2{}^{15}O$-PET,[12,17,19] and DTI.[21-24] Our voxel-based analysis yielded below-normal NAA/Cr In left FPO-CS and its white matter, above-normal Cho/Cr in right FPO-CS and in left FPO-CS white matter. Perhaps these various metabolic aberrations compromise local timing and signal transmission functions.

IPC is the second stage for proprioceptive input in speech.[53] Reduced parietal activation has been documented in stuttering with near-infrared spectroscopy,[54] and shift of activation to the IPC is associated with attainment of fluency in stutterers.[55] Stuttering effects have been noted in IPC with MRI,[1,5] task-fMRI,[7-8] and ^{18}FDG-PET;[20] DTI has detected low FA in inferior parietal white matter.[21-22] Our voxel-based analysis found elevated Cho/Cr in people who stutter in large swaths of **parietal cortex** (not limited to IPC, including also superior parietal cortex), elevated NAA/Cr in large areas of parietal white matter, and low Cho/Cr in inferior parietal white matter. These complex effects await further study.

During speech, the **caudate** is believed to prepare an efferent copy of a feed-forward motor plan and to inhibit projections to sensory from motor cortex.[55] The caudate may be responsible for poor motor timing during speech,[16,56] and for putting out aberrant cues to initiate and to terminate articulatory movements.[44] Right caudate has exhibited below-normal MRI volume,[6] above-normal BOLD activation,[7] and above-normal rCBF[16] in stuttering; left caudate shows below-normal rCBF.[12] Our ROI-analysis found reduced NAA/Cr in right caudate in stutterers that correlated positively with stuttering symptoms. This suggests hypodensity or diminished metabolic activity of neurons in right caudate as attempted compensation for stuttering (less severe symptoms for lower NAA/Cr), perhaps in cooperation with right IFC.

Left **putamen** is responsible for fine-grained movements[12] and may contribute to poor motor timing during speech.[56] A few studies have implicated the left putamen especially in stuttering, with MRI,[4] fMRI,[4,8,12] and rsfMRI.[15] In our ROI- and voxel-based analyses, Cho/Cr in left **putamen** was elevated in stuttering.

The **thalamus**, through the thalamocortical tracts, connects the cortex with the deep brainstem nuclei that control the speech musculature.[40] It has been proposed that low FA in these tracts throws off coordination of speech muscles disturbing the timing, amplitude, and sequence of speech movements.[40] A hyperdopaminergic state was also hypothesized in stuttering in these pathways to undermine speech motor control.[44] Our study observed elevated NAA/Cr in left thalamus and elevated Cho/Cr in both thalami in the stuttering sample in both ROI- and voxel-based analyses. These findings may be consistent with elevated neuronal and glial density and membrane anabolism in these nuclei.

SFC is the second stage for auditory input in speech production.[53] There are numerous prior findings of stuttering-related alterations in SFC using MRI,[4-5] task-fMRI,[7-9] rsfMRI,[13] and ^{18}FDG-PET.[20] In our voxel-based analysis, below-normal NAA/Cr and Cho/Cr were measured in SFC and elevated NAA/Cr was measured in bilateral frontal deep white matter. These findings may reflect lower neuronal and glial density and metabolic activity, or slower membrane metabolism, in the cortex and the reverse in the white matter.

The voxel-based analysis also revealed elevated Cho/Cr in left lateral **temporal cortex** and elevated NAA/Cr in bilateral temporal white matter in stutterers. In bilateral mesial temporal cortex (parahippocampal cortex, hippocampus) NAA/Cr was higher in the stuttering sample. In left hippocampus, Cho/Cr was higher. Findings in these centers are fewer in stuttering. Altered BOLD activation has been observed In left middle temporal cortex[4,9] and in left hippocampus.[9] Finally, voxel-based analysis revealed higher Cho/Cr in people who stutter in bilateral **posterior cingulate cortex**. Above-normal gray-matter volume has been measured in stuttering in these areas,[4] as well as elevated BOLD activation[7-8] and diminished GMR.[20]

Overall, reflecting the complexity of speech production, alterations of neuronal density and metabolism apparently manifest in widespread brain regions responsible for functions in a number of different functional domains, such as motor planning, timing, sequencing, and inhibitory control; auditory spectral decomposition and feedback monitoring; and integration of proprioceptive somatosensory input. Thus, although stuttering is clinically a somewhat focal speech impediment, it has quite diffuse (likely network-distributed) physiological concomitants in the brain, revealing themselves in multiple neuroimaging modalities, including, now, also proton MRS.

Voxel-Based Metabolite Correlations of Metabolite Ratios with Severity of Stuttering Symptom

The voxel-based correlations of NAA/Cr or Cho/Cr with ACES/OASES Section I stuttering severity (eTable 2) were of three kinds:

First, there were positive correlations of NAA/Cr with Section I in left MFC, right STC, left PCC, bilateral deep prefrontal white matter, and bilateral thalamus. In the same vein were positive correlations of Cho/Cr with Section I in bilateral deep prefrontal white matter, and bilateral thalamus. These were all regions where NAA/Cr or Cho/Cr, respectively, was elevated in the stuttering over the control sample in the ROI- or voxel-based analyses. Thus, shifts in neuronal density or metabolic activity, represented by NAA/Cr, or total cell density or membrane metabolism, represented by Cho/Cr, in these regions may foster (or be a consequence of) stuttering symptoms. The functional roles of these brain regions and their circuits, as well as prior neuroimaging evidence of their involvement in stuttering, have been discussed above.

Regarding the positive correlations of NAA/Cr and of Cho/Cr with Section I score in left and right thalamus, the NAA/Cr and Cho/Cr ratios at these two sites were significantly higher in children who stutter than in adults who stutter (eTable 4). Also, children who stutter in our sample had higher Section I scores than adults who stutter (Table 1). Therefore, it is conceivable that the aforementioned positive correlations represent mere byproducts of a normal age-related drop in NAA/Cr and Cho/Cr, combined with the happenstance of high symptoms in this particular child shuttering subcohort. This interpretation, however, is not supported by the observation that thalamic NAA/Cr and Cho/Cr are nearly identical in the child and adult control sample (eTable 4), arguing against the existence of a drop in NAA/Cr and Cho/Cr in the normal transition from child to adult. Moreover, the higher Section I scores among children in our stuttering sample are probably not fortuitous, as they are consistent with the commonly observed attenuation of severity with age in stuttering,[67] One might argue instead for declines in thalamic NAA/Cr and Cho/Cr as possible metabolic signs of processes contributing to this frequently observed symptomatic relief in the neurodevelopmental course of stuttering.

Second, there were a few regions demonstrating elevated or diminished metabolite ratios in the stuttering sample in the ROI- or voxel-based analyses, where the correlation ran in the opposite direction to the diagnostic effect. Thus, in bilateral FpC, NAA/Cr and Cho/Cr were diminished in the stuttering group, but the correlations of NAA/Cr and Cho/Cr with Section I were positive. In right STC, Cho/Cr was higher in the stuttering group, but the correlation of Cho/Cr with Section I was negative. In latPC, NAA/Cr and Cho/Cr correlated negatively with Section I, but (at least in right latPC) these ratios were elevated in the stuttering sample. And in bilateral amygdala, NAA/Cr and Cho/Cr were elevated in the stuttering group, but correlated negatively with Section I. Such "wrong-way" correlations (e.g., the oft-cited IFC correlation reported by Preibisch[41]) may reflect adaptations of remote brain regions in attempted compensation for functional deficits in the primary regions afflicted in stuttering. Such adaptations are common across neurodevelopmental disorders[57] and have been a particular recurring theme in the neuroimaging of stuttering.[8,12,16-17] We observed multiple such apparent compensatory effects in our fMRI study of stuttering.[7] Results of the present MRS study suggest that metabolic reorganization in bilateral FpC, as well as metabolic shifts in the opposite direction in bilateral latPC and amygdala and right STC, represent imperfect efforts to compensate for deficiencies in other brain regions.

Third, several significant correlations between NAA/Cr and/or Cho/Cr and Section I were recorded in brain regions where no significant effect of stuttering diagnosis was registered. These included positive correlations of NAA/Cr with Section I in left IFC, right inferior temporal cortex, bilateral lingual cortex, right anterior middle cingulate cortex, right posterior middle cingulate cortex, and left deep temporal white matter. There were positive correlations of Cho/Cr with Section I in left MFC, right inferior temporal cortex, bilateral lingual cortex, and right anterior middle cingulate cortex. Finally, there were negative correlations of NAA/Cr and Cho/Cr in right forceps minor. Some of these regions were sites of diagnostic effects of stuttering or symptom correlations in our fMRI study.[7] In particular, we observed above-normal BOLD activation during conflict-resolution in anterior middle cingulate cortex and correlations with stuttering severity in anterior and posterior middle cingulate cortices (together labeled "ACC"), while below-normal BOLD signal was observed in left IFC and MFC (together labeled "DLPFC"). Left IFC and MFC also belong to the Bohland[58] speech network and the Jürgens[53] speech-production network. The latter also contains the anterior middle cingulate cortex, the function of which include volitional initiation and suppression of emotional states and innate motor patterns. Metabolic disturbance in this center might thus directly contribute to stuttering symptoms. Piai[59] documented a BOLD activation of bilateral (but especially right) posterior middle cingulate cortex (which they call "dorsal anterior cingulate"), which was interpreted as control over speech production as part of its domain-general attention-control function. Left IFC is, famously, Broca's area executing phonetic encoding and articulatory programming. Among other effects, below-normal volumes of left IFC have been measured in children[22] and adults,[8] and elevated rsBOLD[13] have been recorded in left IFC, in stuttering persons. With the present investigation, an association of elevated NAA/Cr with stuttering severity joins this list of neuroimaging signs. Although the lingual gyri are typically associated with vision, they also exhibit BOLD or rCBF activation during the naming of stimuli,[60-62] during retrieval of words[63] and in verbalizing high-emotion *vs.* emotionally neutral words,[64] all common vocal contexts for stuttering. The last two effects have been linked to hippocampal, respectively, amygdalar function, recalling our above findings of elevated NAA/Cr and Cho/Cr in stuttering in the emotional-memory network. As also mentioned, DTI has previously identified disturbances in numerous white-matter regions in stuttering.[5,21-24] Relatively few neuroimaging effects of stuttering are documented in right inferior temporal cortex.[4,65] Overall, the present MRS symptom-correlation results fortify and enlarge the conception of the neurophysiology of stuttering emerging from prior imaging (including our fMRI investigation) and speech-production models.

ROI-Based Effects on Regional Metabolite Ratios in Children *vs.* Adults

Several diagnostic metabolite effects of stuttering were significant within the child subsample only, including diminished NAA/Cr in right IFC and elevated NAA/Cr in left insula and bilateral thalamus, as well as elevated Cho/Cr in bilateral thalamus. For left and right thalamic NAA/Cr and right thalamic Cho/Cr, these markers were also larger in child than adult people with stuttering. There was a further observation of lower NAA/Cr in right MFC and left insula in child than adult people with stuttering. Metabolite ratios were higher in children than adults in the control sample only in several brain regions, including NAA/Cr in right STC, NAA/Cr and Cho/Cr in right FPO-CS white matter, and NAA/Cr and Cho/Cr in right inferior parietal white matter. In only one region, right STC, were metabolite effects (higher NA/Cr and Cho/Cr) detected only in adults who stutter. To the extent that one can infer from cross-sectional data, these results are supportive of somewhat different metabolic profiles in children *vs.* adults who stutter and of maturational alterations from childhood to adulthood in shuttering.

ROI-Based Effects on Regional Metabolite Ratios in Males *vs.* Females

All told, relatively few significant stuttering-related differences were demonstrated between males and females, these being localized to right STC and right putamen. While stuttering is clearly much more common in males[66] our MRS study was scarcely able to identify brain bases possibly contributing to this epidemiological observation.

eFigure 1. T1-Weighted Brain MRI With A Priori Targeted Regions of Interest (ROIs)

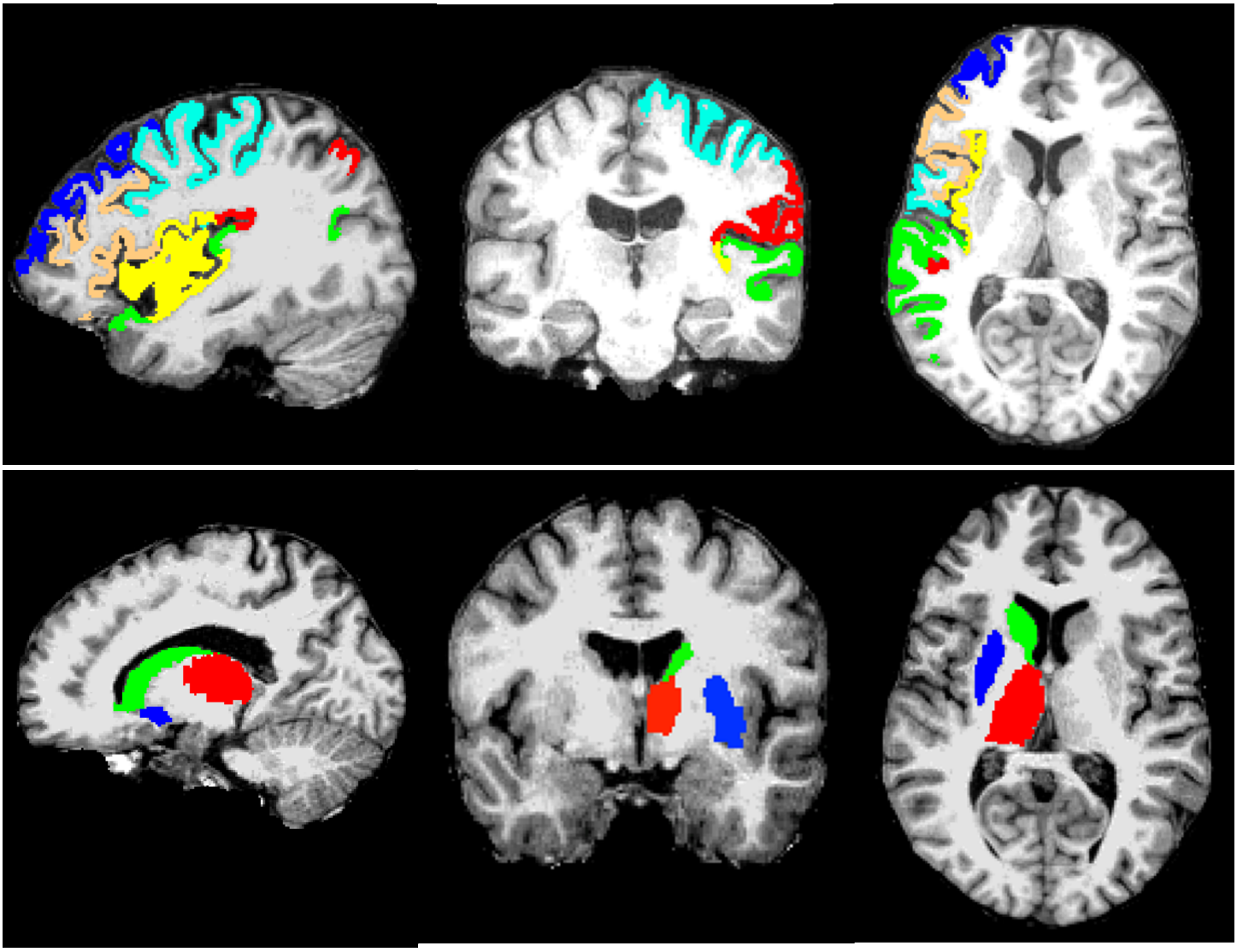

Sagittal, coronal, and axial-oblique (AC-PC parallel) MRI sections displaying cortical (upper) and subcortical (lower) ROIs. Color-code for cortical ROIs: blue—middle frontal cortex, copper—inferior frontal cortex, yellow—insular cortex, green—superior temporal cortex, turquoise—frontoparietal opercular-central sulcal cortex, red—inferior parietal cortex; for subcortical nuclei: green—caudate, blue—putamen, red—thalamus.

eFigure 2. Selected Voxel-Based Maps for NAA/Cr and Cho/Cr Correlations With ACES/OASES Section I Stuttering Severity Score

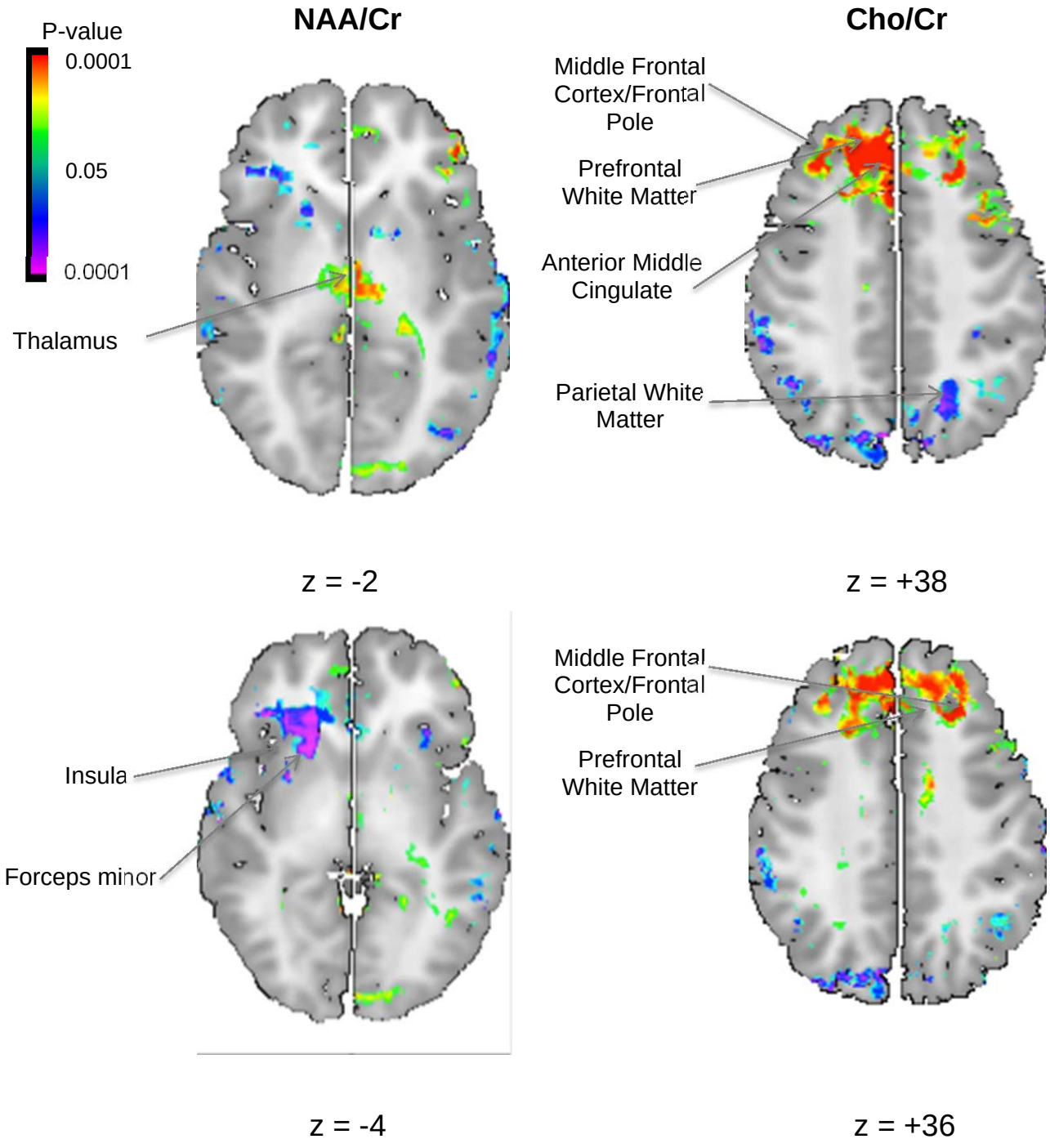

Axial-oblique brain MRI sections in radiologic convention at selected MNI152 z (superior-inferior) levels showing regions where mean metabolite ratio within the stuttering sample correlated positively (red-yellow), respectively, negatively (blue-purple) with ACES/OASES Section I score (FDR-corrected). Voxel-based analyses performed on usable data from 43 stuttering and 50 control participants.

eTable 1. Combination ROIs Used in ROI-Based Metabolite Ratio Analysis

Combination ROI	Constituent Destrieux Labels	Number	aseg/aparc2009 Designation
middle frontal cortex	middle frontal gyral cortex	11115	ctx_lh_G_front_middle
	middle frontal cortex in inferior frontal sulcus	11154	ctx_lh_S_front_middle
inferior frontal cortex	inferior frontal gyrus pars orbitalis	11113	ctx_lh_G_front_inf-Orbital
	cortex inside lateral sulcus horizontal ramus	11139	ctx_lh_Lat_Fis-ant-Horizont
	inferior frontal gyrus pars triangularis	11114	ctx_lh_G_front_inf-Triangul
	cortex inside lateral sulcus vertical ramus	11140	ctx_lh_Lat_Fis-ant-Vertical
	inferior frontal gyrus pars opercularis	11112	ctx_lh_G_front_inf-Opercular
	inferior frontal cortex in inferior frontal sulcus	11153	ctx_lh_S_front_inf
insular cortex	circular sulcal cortex ant	11148	ctx_lh_S_circular_insula_ant
	anterior insular cortex	11118	ctx_lh_G_insular_short
	posterior insular cortex	11117	ctx_lh_G_Ins_lg_and_S_cent_ins
	circular sulcal cortex inferior	11149	ctx_lh_S_circular_insula_inf
	circular sulcal cortex superior	11150	ctx_lh_S_circular_insula_sup
superior temporal cortex	lateral superior temporal cortex	11134	ctx_lh_G_temp_sup-Lateral
	cortex inside superior temporal sulcus	11174	ctx_lh_S_temporal_sup
	planum polare	11135	ctx_lh_G_temp_sup-Plan_polar
	transverse temporal cortex	11133	ctx_lh_G_temp_sup-G_T_transv
	transverse temporal sulcal cortex	11175	ctx_lh_S_temporal_transverse
	planum temporale	11136	ctx_lh_G_temp_sup-Plan_tempo
frontoparietal opercular—	cortex inside precentral sulcus inferior part	11169	ctx_lh_S_precentral-inf-part
central sulcal cortex	cortex inside precentral sulcus superior part	11170	ctx_lh_S_precentral-sup-part
	precentral gyral cortex	11129	ctx_lh_G_precentral
	cortex inside central sulcus	11146	ctx_lh_S_central
	subcentral gyral cortex (inferior *pli de passage*)	11104	ctx_lh_G_and_S_subcentral
	paracentral cortex (superior *pli de passage*)	11103	ctx_lh_G_and_S_paracentral
	post-central gyral cortex	11128	ctx_lh_G_postcentral
	cortex inside postcentral sulcus	11168	ctx_lh_S_postcentral
inferior parietal cortex	supramarginal gyral cortex	11126	ctx_lh_G_pariet_inf-Supramar
	cortex inside posterior segment of lateral sulcus	11141	ctx_lh_Lat_Fis-post
	angular gyral cortex	11125	ctx_lh_G_pariet_inf-Angular
caudate	caudate nucleus	11	Left-Caudate
putamen	putamen	12	Left-Putamen
thalamus	thalamus	9	Left-Thalamus

For each cortical ROI, a corresponding white-matter ROI was generated out of the white matter underlying each of the constituent ROIs. A right-hemisphere homolog of each ROI was also generated. Labels and designations from Destrieux.[25]

eTable 2. Group Mean (SD) Regional Metabolite Ratios for Stuttering and Control Samples

	Left Hemisphere			Right Hemisphere		
	Stuttering	**Control**	***P*-Value**	**Stuttering**	**Control**	***P*-Value**
			NAA/Cr			
Cortical regions						
Middle frontal (L62,R66)	1.58 (0.36)	1.74 (0.42)	0.12	1.72 (0.36)	1.82 (0.44)	0.24
Inferior frontal (L74,R73)	1.72 (0.25)	1.81 (0.37)	0.16	1.83 (0.27)	1.97 (0.23)	**0.018**[a]
Insular (L65,R62)	1.96 (0.27)	1.94 (0.32)	0.81	1.90 (0.33)	1.88 (0.28)	0.50
Superior temporal (L76,R76)	1.95 (0.25)	1.89 (0.34)	0.39	2.04 (0.29)	1.93 (0.37)	0.10
Frontoparietal opercular-central sulcal (L74,R72)	1.78 (0.32)	1.82 (0.32)	0.50	2.06 (0.27)	2.13 (0.35)	0.31
Inferior parietal (L68,R70)	1.86 (0.42)	1.93 (0.49)	0.64	2.13 (0.27)	2.11 (0.42)	0.70
White-matter regions						
Middle frontal (L38,R51)	1.86 (0.34)	1.95 (0.44)	0.40	1.91 (0.29)	2.05 (0.39)	0.14
Inferior frontal (L65,R70)	1.92 (0.25)	1.95 (0.39)	0.78	1.98 (0.24)	2.23 (0.31)	**0.005**[a]
Insular (L61,R60)	2.19 (0.31)	2.30 (0.37)	0.20	2.16 (0.29)	2.29 (0.30)	0.056
Superior temporal (L73,R71)	2.27 (0.29)	2.20 (0.42)	0.49	2.27 (0.23)	2,20 (0.40)	0.28
Frontoparietal opercular-central sulcal (L74,R72)	2.11 (0.28)	2.16 (0.32)	0.43	2.24 (0.24)	2.27 (0.32)	0.67
Inferior parietal (L64,R57)	2.35 (0.33)	2.27 (0.48)	0.44	2.31 (0.31)	2.35 (0.41)	0.61
Subcortical nuclei						
Caudate (L43,R45)	1.73 (0.38)	1.76 (0.46)	0.75	1.66 (0.25)	1.86 (0.35)	**0.04**[b]
Putamen (L72,R72)	1.85 (0.31)	1.87 (0.27)	0.70	1.77 (0.28)	1.83 (0.20)	0.25
Thalamus (L74,R76)	1.86 (0.33)	1.73 (0.23)	**0.04**[b]	1.73 (0.32)	1.65 (0.21)	0.22
			Cho/Cr			
Cortical regions						
Middle frontal (L64,R67)	0.75 (0.17)	0.83 (0.24)	0.15	0.86 (0.17)	0.86 (0.17)	0.91
Inferior frontal (L74,R73)	0.89 (0.19)	0.84 (0.16)	0.32	0.96 (0.14)	0.94 (0.12)	0.48
Insular (L65,R62)	1.31 (0.21)	1.29 (0.20)	0.66	1.26 (0.14)	1.25 (0.18)	0.72
Superior temporal (L76,R76)	1.03 (0.16)	0.94 (0.20)	**0.03**[b]	1.05 (0.16)	0.94 (0.20)	**0.01**[b]
Frontoparietal opercular-central sulcal (L74,R72)	0.81 (0.15)	0.81 (0.14)	0.95	0.91 (0.13)	0.92 (0.17)	0.66
Inferior parietal (L68,R72)	0.90 (0.23)	0.92 (0.22)	0.63	1.03 (0.19)	0.99 (0.22)	0.43
White-matter regions						
Middle frontal (L39,R52)	1.00 (0.20)	1.11 (0.25)	0.12	1.07 (0.15)	1.16 (0.21)	**0.04**
Inferior frontal (L65,R70)	0.98 (0.16)	0.92 (0.16)	0.16	1.05 (0.13)	1.06 (0.12)	0.77
Insular (L62,R60)	1.23 (0.17)	1.17 (0.19)	0.21	1.24 (0.14)	1.19 (0.14)	0.14
Superior temporal (L73,R72)	1.23 (0.17)	1.08 (0.26)	**0.003**[b]	1.21 (0.15)	1.11 (0.24)	**0.02**[b]
Frontoparietal opercular-central sulcal (L74,R72)	1.03 (0.15)	0.98 (0.16)	0.17	1.08 (0.14)	1.05 (0.19)	0.49
Inferior parietal (L64,R57)	1.25 (0.23)	1.12 (0.25)	**0.04**	1.22 (0.18)	1.18 (0.24)	0.44
Subcortical nuclei						
Caudate (L43,R45)	1.19 (0.23)	1.12 (0.26)	0.37	1.20 (0.20)	1.16 (0.19)	0.75
Putamen (L72,R72)	1.28 (0.18)	1.17 (0.17)	**0.01**[b]	1.77 (0.18)	1.13 (0.15)	0.34
Thalamus (L74,R76)	1.19 (0.17)	1.07 (0.17)	**0.002**[b]	1.18 (0.16)	1.06 (0.14)	**0.001**[b]

Abbreviations: SD, standard deviation; NAA, *N*-acetyl-aspartate+*N*-acetyl-aspartyl-glutamate; Cr, creatine+phosphocreatine; Cho, choline-containing compounds. Significant effects in **bold**. (Degrees-of-freedom for each region and hemisphere in parentheses.)

[a] $P < 0.05$ for *post-hoc* protected analysis-of-covariance covarying Sex, Age, and gray matter following omnibus repeated-measures multivariate analysis-of-variance.

[b] $P < 0.05$ for *post-hoc* protected analysis-of-covariance covarying Sex and Age following omnibus repeated-measures multivariate analysis-of-variance.

eTable 3. Voxel-Based CSI Metabolite-Symptom Correlations in Stuttering Sample (Section 1)

	Positive Correlation With Section I Score			
	NAA/Cr		Cho/Cr	
Brain Region	**(x,y,z)**	**P**	**(x,y,z)**	**P**
	also ROI-based regions			
Left middle frontal cortex	-42,6,36	0.005	-42,30,38	<0.001
Left inferior frontal cortex	-42,12,26	<0.001		
Left thalamus	-8,-18,-2	<0.001	-8,-14,-2	0.005
Right thalamus	10,-14,-2	0.006	8,-14,2	0.01
	non-ROI-based regions			
Left frontopolar cortex	-28,42,36	<0.001	-28,38,36	<0.001
Right frontopolar cortex	24,40,36	<0.001	26,34,38	<0.001
Right inferior temporal cortex	44,-56,-10	<0.001	44,-56,-10	<0.001
Left lingual cortex	-22,-58,-12	0.006	-22,-64,-12	0.004
Right lingual cortex	24,-56,-10	0.001	26,-52,-10	<0.001
Right anterior middle cingulate cortex	8,20,36	<0.001	6,22,38	<0.001
Right posterior middle cingulate cortex	4,-10,34	<0.001		
Left posterior cingulate cortex††	-8,-48,34	0.01		
Left deep prefrontal white matter	-14,38,36	<0.001	-14,34,36	<0.001
Right deep prefrontal white matter	14,30,38	<0.001	16,28,38	<0.001
Left deep temporal white matter	-34,-56,-12	0.005		
	Negative Correlation With Section I Score			
	NAA/Cr		**Cho/Cr**	
	also ROI-based regions			
Right insula	32,24,-2	<0.001	32,18,-6	<0.001
Right superior temporal cortex	60,-10,-4	<0.001	60,-14,-8	<0.001
	non-ROI-based regions			
Left lateral parietal cortex†	-32,-58,48	<0.001	-36,-56,48	<0.001
Right lateral parietal cortex†	34,-42,46	<0.001	34,-48,46	<0.001
Left amygdala	-10,-8,-16	<0.001	-12,-8,-16	<0.001
Right amygdala	20,-6,-16	<0.001	18,-6,-16	<0.001
Right forceps minor	20,30,-2	<0.001	34,34,2	<0.001
Right deep prefrontal white matter			26,28,-6	<0.001
Left deep parietal white matter			-20,-56,38	<0.001

Italics: regions also tested with ROI-based analysis; **bold** region showed significant ROI-based symptom correlation
†"lateral parietal cortex" comprises inferior frontal and lateral superior frontal cortices
††"posterior cingulate cortex" comprises dorsal and ventral posterior cingulate cortices
Abbreviations: NAA, *N*-acetyl-aspartate+*N*-acetyl-aspartyl-glutamate; Cr, creatine+phosphocreatine; Cho, choline-containing compounds; (x,y,z), MNI152-coordinates with regional assignments *per* the Harvard-Oxford Atlas.[34]
P–values for FDR-corrected Pearson correlation.
Voxel-based analyses performed on usable data from 43 stuttering and 50 control participants.

eTable 4. ROI-Based Effects on Regional Metabolite Ratios in Children vs Adults

	Child					Adult		
	Stuttering	***P*-Value[a]**	***P*-Value[b]**	**Control**	***P*-Value[c]**	**Stuttering**	***P*-Value[d]**	**Control**
				NAA/Cr				
R MFC	**1.58 (0.31)**	0.12	**0.02**	1.77 (0.38)	0.48	1.87 (0.36)	0.95	1.88 (0.50)
R IFC	**1.79 (0.28)**	**0.02**	0.16	1.98 (0.23)	0.85	1.88 (0.25)	0.30	1.96 (0.23)
L insula	**2.09 (0.23)**	**0.05**	**0.02**	1.92 (0.29)	0.51	1.81 (0.24)	0.16	1.98 (0.38)
R STC	2.08 (0.28)	0.65	0.47	**2.11 (0.23)**	**0.04**	**2.01 (0.31)**	**0.03**	1.74 (0.40)
R FPO-CSWM	2.28 (0.22)	0.88	0.36	**2.37 (0.30)**	**0.05**	2.20 (0.27)	0.77	2.17 (0.32)
R IPWM	2.27 (0.32)	0.93	0.46	**2.52 (0.35)**	**0.05**	2.35 (0.32)	0.34	2.22 (0.42)
L Thalamus	**2.02 (0.34)**	**0.006**	**0.02**	1.75 (0.24)	0.39	1.67 (0.21)	0.64	1.70 (0.22)
R Thalamus	**1.90 (0.33)**	**0.009**	**<0.001**	1.64 (0.25)	0.96	1.54 (0.18)	0.32	1.65 (0.16)
				Cho/Cr				
R STC	1.06 (0.19)	0.58	0.53	1.04 (0.12)	0.076	**1.03 (0.11)**	**0.004**	0.86 (0.23)
R FPO-CS	0.91 (0.14)	0.91	0.84	**0.99 (0.12)**	**0.02**	0.92 (0.12)	0.39	0.84 (0.19)
R FPO-CSWM	1.10 (0.16)	0.33	0.28	**1.13 (0.16)**	**0.005**	1.05 (0.10)	0.088	0.97 (0.18)
R IPWM	1.18 (0.18)	0.44	0.23	**1.29 (0.22)**	**0.05**	**1.26 (0.17)**	**0.03**	1.10 (0.23)
L Thalamus	**1.25 (0.17)**	**0.003**	0.08	1.08 (0.15)	0.65	1.12 (0.14)	0.18	1.05 (0.18)
R Thalamus	**1.24 (0.17)**	**0.002**	**0.01**	1.07 (0.15)	0.53	1.11 (0.13)	0.13	1.05 (0.13)

Bold regions showed significant mean differences in comparisons between subgroups

Abbreviations: NAA, *N*-acetyl-aspartate+*N*-acetyl-aspartyl-glutamate; Cr, creatine+phosphocreatine; Cho, choline-containing compounds; L, left; R, right; MFC, middle frontal cortex; IFC, inferior frontal cortex; STC, superior temporal cortex; FPO-CS, frontoparietal-opercular-central sulcal cortex; FPO-CSWM, frontoparietal-opercular-central sulcal white matter; IPWM, inferior parietal white matter

a stuttering *vs.* control within child sample (T-test or ANCOVA covarying tissue content).

b children *vs.* adults within stuttering sample (T-test or ANCOVA covarying tissue content).

c children *vs.* adults within control sample (T-test or ANCOVA covarying tissue content).

d stuttering *vs.* control within adult sample (T-test or ANCOVA covarying tissue content).

eTable 5. ROI-Based Effects on Regional Metabolite Ratios in Males vs Females

	Female				Male	
	Stuttering	***P*-Value[a]**	***P*-Value[b]**	**Control**	**Stuttering**	**Control**
			NAA/Cr			
Right superior temporal cortex	**2.20 (0.26)**	**0.03**	**0.006**	2.02 (0.37)	1.94 (0.26)	1.86 (0.37)
			Cho/Cr			
Right putamen	**1.09 (0.15)**	0.58	**0.03**	1.10 (0.10)	1.21 (0.19)	1.15 (0.18)

Bold regions showed significant mean differences in comparisons between subgroups

Abbreviations: NAA, *N*-acetyl-aspartate+*N*-acetyl-aspartyl-glutamate; Cr, creatine+phosphocreatine; Cho, choline compounds.

a stuttering *vs.* control within female sample (T-test or ANCOVA covarying tissue content).

b female *vs.* male within stuttering sample (T-test or ANCOVA covarying tissue content).

eReferences

1. Beal DS, Gracco VL, Brettschneider J, Kroll RM, De Nil LF. A voxel-based morphometry (VBM) analysis of regional grey and white matter volume abnormalities within the speech production network of children who stutter. *Cortex*. 2013;49:2151–2161.

2. Chang EF, Niziolek CA, Knight RT, Nagarajan SS, Houde JF. Human cortical sensorimotor network underlying feedback control of vocal pitch. *Proc Natl Acad Sci USA*. 2013;110:2653–2658.

3. Chang S-E, Kenney MK, Loucks TMJ, Ludlow CL. Brain activation abnormalities during speech and non-speech in stuttering speakers. *NeuroImage*. 2009;46:201–12.

4. Lu C, Peng D, Chen C, et al. Altered effective connectivity and anomalous anatomy in the basal ganglia-thalamocortical circuit of stuttering speakers. *Cortex*. 2010;46:49–67.

5. Chang S-E, Erickson KI, Ambrose NG, Hasegawa-Johnson MA, Ludlow CL. Brain anatomy differences in childhood stuttering. *NeuroImage*. 2008;39:1333–44.

6. Foundas AL, Cindass R Jr, Mock JR Corey DM. Atypical caudate anatomy in children who stutter. *Neurology Percpt Motor Skills: Phys Devel Measurement*. 2013;116(2):528–543.

7. Liu J, Wang Z, Huo Y, et al. A functional imaging study of self-regulatory capacities in persons who stutter. *PloS ONE*. 2014;9(2):e89891.

8. Kell CA, Neumann K, von Kriegstein K, et al. How the brain repairs stuttering. *Brain*. 2009;132:2747–60.

9. Belyk M, Kraft SJ, Brown S. Stuttering as a trait or state—an ALE meta-analysis of neuroimaging studies. *Eur J Neurosci*. 2015;41:275–84.

10. Giraud A-L, Neumann K, Bachoud-Levi A-C, et al. Severity of dysfluency correlates with basal ganglia activity in persistent developmental stuttering. *Brain Lang*. 2008;104:190–199.

11. Neumann K, Preibisch C, Euler HA, et al. Cortical plasticity associated with stuttering therapy. *J Fluen Disord*. 2005;30:23–39.

12. Ingham RJ, Grafton ST, Bothe AK, Ingham JC. Brain activity in adults who stutter: similarities across speaking tasks and correlations with stuttering frequency and speaking rate. *Brain Lang*. 2012;122:11–24.

13. Xuan Y, Meng C, Yang Y, et al. Resting-state brain activity in adult males who stutter. *PLos ONE*. 2012;7(1):e30570.

14. Chang S-E, Horwitz B, Ostuni J, Reynolds R, Ludlow CL. Evidence of left inferior frontal–premotor structural and functional connectivity deficits in adults who stutter. *Cereb Cortex*. 2011;21:2507–18.

15. Chang SE, Zhu DC. Neural network connectivity differences in children who stutter. *Brain* 2013;136:3709–3726.

16. Braun AR, Varga M, Stager S, et al. Altered patterns of cerebral activity during speech and language production in developmental stuttering. An $H_2{}^{15}O$ positron emission tomography study. *Brain*. 1997;120:761–784.

17. Fox PT, Ingham RJ, Ingham JC, et al. A PET study of the neural systems of stuttering. *Nature*. 1996;382:158–162.

18. Ingham RJ., Fox PT, Ingham JC, et al. Brain correlates of stuttering and syllable production: Gender comparison and replication. *J Speech Lang Hear Res.* 2004;47(2):321-341.

19. De Nil LF, Kroll RM, Kapur S, Houle S. A positron emission tomography study of silent and oral single word reading in stuttering and nonstuttering adults. *J Speech Lang Hear Res*. 2000;43:1038–53.

20. Wu JC, Maguire G, Riley G, et al. A positron emission tomography [^{18}F]deoxyglucose study of developmental stuttering. *Neuroreport.* 1995;6:501–505.

21. Connally EL, Ward D, Howell P, Watkins KE. Disrupted white matter in language and motor tracts in developmental stuttering. *Brain Lang*. 2014;131:25–35.

22. Chang S-E, Zhu DC, Choo AL, Angstadt M.White matter neuroanatomical differences in young children who stutter. *Brain*. 2015;138:694–711.

23. Sommer M, Koch MA, Paulus W, Weiller C, Büchel C. Disconnection of speech-relevant brain areas in persistent developmental stuttering. *Lancet*. 2002;360:380–383.

24. Watkins KE, Smith SM, Davis S, Howell P. Structural and functional abnormalities of the motor system in developmental stuttering. *Brain*. 2008;131:50–59.

25. Destrieux C, Fischl B, Dale A, Halgren E. Automatic parcellation of human cortical gyri and sulci using standard anatomical nomenclature. *Neuroimage*. 2010;53(1):1–15.

26. Hao X, Xu D, Bansal R, et al. Multimodal magnetic resonance imaging: The coordinated use of multiple, mutually informative probes to understand brain structure and function. *Hum Brain Mapp.* 2011;34(2):253-271.

27. Goh S, Dong Z, Zhang Y, DiMauro S, Peterson BS. Mitochondrial dysfunction as a neurobiological subtype of autism spectrum disorder: Evidence from brain imaging. *JAMA Psychiatry*. 2014;71(6):665-671.

28. Dong Z, Peterson B. The rapid and automatic combination of proton MRSI data using multi-channel coils without water suppression. *Magnetic Resonance Imaging*. 2007; 25,1148-1154.

29. Dong Z, Liu F, Kangarlu A, Peterson BS. Metabolite mapping with extended brain coverage using a fast multi-section MRSI pulse sequence and a multi-channel coil. *Int J Biomed Imaging.* 2012; 2012:247161.

30. Dong Z. Proton MRS and MRSI of the brain without water suppression. *Prog NMR Spec*. 2015; 86-87:65-79.

31. Bansal R, Staib LH, Wang Y, Peterson BS. ROC-based assessments of 3D cortical surface-matching algorithms. *Neuroimage*. 2005;24:150–162.

32. de Beer R, van den Boogaart A, van Ormondt D, et al. Application of time-domain fitting in the quantification of In vivo 'H spectroscopic imaging data sets. *NMR Biomed.* 1992;5:171-178.

33. Mueller SG, Ebel A, Barakos J, et al. Widespread extrahippocampal NAA/(Cr+Cho) abnormalities in TLE with and without mesial temporal sclerosis. *J Neurol.* 2011;258:603-612.

34. Desikan RS, Ségonne F, Fischl B, et al. An automated labeling system for subdividing the human cerebral cortex on MRI scans into gyral based regions of interest. *Neuroimage.* 2006;31(3):968-80.

35. Fuster JM. Upper processing stages of the perception-action cycle. *Trends Cogn Sci*. 2004;8:143–145.

36. Geiser E, Notter M, Gabrieli JD. A corticostriatal neural system enhances auditory perception through temporal context processing. *J Neurosci.* 2012;32:6177–6182.

37. Wiener M, Turkeltaub P, Coslett HB. The image of time: a voxel-wise meta-analysis. *Neuroimage.* 2010;49:1728–1740.

38. Toyomura A, Fujii T, Kuriki S. Effect of external auditory pacing on the neural activity of stuttering speakers. *NeuroImage*. 2011;57:1507–1516.

39. Etchell AC, Johnson BW, Sowman PF. Behavioral and multimodal neuroimaging evidence for a deficit in brain timing networks in stuttering: a hypothesis and theory. *Fron Hum Neurosci*. 2014;8(467):1-10.

40. Chang S-E. Research updates in neuroimaging studies of children who stutter. *Sem Speech Lang*. 2014;35(2):67-79.

41. Preibisch C, Neumann K, Raab P, et al. Evidence for compensation for stuttering by the right frontal operculum. *NeuroImage*. 2003;20:1356–64.

42. Brown S, Ingham RJ, Ingham JC, Laird AR, Fox PT. Stuttered and fluent speech production: an ALE meta-analysis of functional neuroimaging studies. *Hum Brain Mapp.* 2005;25: 05–117.

43. Ingham RJ, Ingham JC, Finn P, Fox PT. Towards a functional neural systems model of developmental stuttering. *J Fluency Disord.* 2003;28:297–317; quiz 317–298.

44. Craig-McQuiade A, Akram H, Zrinzo L, Tripoliti E. A review of brain circuitries involved in stuttering. *Fron Hum Neurosci*. 2014;8(884):1-20.

45. Rauch SL, Savage CR, Alpert NM, Fischman AJ, Jenike MA. The functional neuroanatomy of anxiety: A study of three disorders using positron emission tomography and symptom provocation. *Biol Psychiatry*. 1997;42:446–452.

46. Hashimoto Y, Sakai KL. Brain activations during conscious self- monitoring of speech production with delayed auditory feedback: an fMRI study. *Hum Brain Mapp*. 2003;20:22–28.

47. Fu CH, Vythelingum GN, Brammer MJ, et al. An fMRI study of verbal self-monitoring: neural correlates of auditory verbal feedback. *Cereb Cortex.* 2006;16:969–977.

48. Wilson SM, Galantucci S, Tartaglia MC, et al. Syntactic processing depends on dorsal language tracts. *Neuron*. 2011;72:397–403.

49. Sarubbo S, De Benedictis A, Merler S, et al. Towards a functional atlas of human whitematter. *Hum Brain Mapp.* 2015;36:3117-3136.

50. Friederici AD. The cortical language circuit: from auditory perception to sentence comprehension. *Trends Cogn Sci*. 2012;16:262–268.

51. Fox PT. Brain imaging in stuttering: where next? *J Fluency Disord*. 2003;28:265-272.

52. Weiler N, Wood L, Yu J, Solla SA, Shepherd GMG. Top-down laminar organization of the excitatory network in motor cortex. *Nat Neurosci*. 2008;11:360–366.

53. Jürgens U. Neural pathways underlying vocal control. *Neurosci Biobehav Rev.* 2002;26:235–258.

54. Sato Y, Mori K, Koizumi T, et al. Functional lateralization of speech processing in adults and children who stutter. *Fron Psychol*. 2011;2(70):1-10.

55. Neef E, Anwander A, Friederici AD. The neurobiological grounding of persistent stuttering: from structure to function. *Curr Neurol Neurosci Rep*. 2015;15(63):1-11.

56. Alm PA. Stuttering and the basal ganglia circuits: A critical review of possible relations. *J Comm Disord*. 2004;37(4):325-369.

57. Marsh R, Maia TV, Peterson BS. Functional disturbances within frontostriatal circuits across multiple childhood psychopathologies. *Am J Psychiatry*. 2009;166(6):664-674.

58. Bohland JW, Bullock D, Guenther FH. Neural representations and mechanisms for the performance of simple speech sequences. *J Cogn Neurosci*. 2009;22:1504–1529.

59. Piai V, Roelofs A, Acheson DJ, Takashima A. Attention for speaking: domain-general control from the anterior cingulate cortex in spoken word production. *Fron Hum Neurosci*. 2013;7:832.

60. Howard D, Patterson K, Wise R, et al. The cortical localization of the lexicons: positron emission tomography evidence. *Brain.* 1992;115:1769-1782.

61. Bookheimer SY, Zefro TA, Blaxton T, Gaillard W, Theodore W. Regional cerebral blood flow during object naming and word reading. *Hum Brain Mapp.* 1995;3:93-106.

62. Price CJ, Wise R, Watson J, Patterson K, Howard D, Frackowiak RSJ. Brain activity during reading: the effects of task and exposure duration. *Brain.* 1994;117:1255-1269.

63. Cho S, Metcalfe AWS, Young CB, Ryali S, Geary DC, Menon V. Hippocampal-prefrontal engagement and dynamic causal interactions in the maturation of children's fact retrieval. *J Cog Neurosci*. 2012;24(9):1849-1866.

64. Isenberg N, Silbersweig D, Engelien A, et al. Linguistic threat activates the human amygdala. *PNAS USA.* 1999;96(18):10456-10459.

65. Toyomura A, Fujii T, Kuriki S. Effect of an 8-week practice of externally triggered speech on basal-ganglia activity of stuttering and fluent speakers. *NeuroImage*. 2015;109:458–468.

66. Halpern DF. *Sex Differences in Cognitive Abilities.* Mahwah, NJ: Lawrence Erlbaum Associates; 2000.

67. Yairi E, Ambrose N. Epidemiology of stuttering: 21st century advances. *J Fluency Disord.* 2013;38:66–87.